X. Liu
Institute of Solid Mechanics,
Beijing University of Aeronautics
and Astronautics,
Beijing 100191, China
e-mail: liuxia@lnm.imech.ac.cn

Z. X. Lu
Institute of Solid Mechanics,
Beijing University of Aeronautics
and Astronautics,
Beijing 100190, China
e-mail: luzixing@buaa.edu.cn

Y. Chen
State Key Laboratory of Nonlinear Mechanics,
Institute of Mechanics,
Chinese Academy of Science,
Beijing 100190, China;
School of Engineering Science,
University of Chinese Academy of Sciences,
Beijing 101408, China
e-mail: chenyan@lnm.imech.ac.cn

Y. L. Sui
Pipeline Research Institute of China National
Petroleum Corporation,
Langfang Hebei 065000, China
e-mail: suiyl1970@126.com

L. H. Dai[1]
State Key Laboratory of Nonlinear Mechanics,
Institute of Mechanics,
Chinese Academy of Science,
Beijing 100190, China;
School of Engineering Science,
University of Chinese Academy of Sciences,
Beijing 101408, China
e-mail: lhdai@lnm.imech.ac.cn

Improved *J* Estimation by GE/EPRI Method for the Thin-Walled Pipes With Small Constant-Depth Circumferential Surface Cracks

Application of thin-walled high strength steel has become a trend in the oil and gas transportation system over long distance. Failure assessment is an important issue in the construction and maintenance of the pipelines. This work provides an engineering estimation procedure to determine the J-integral for the thin-walled pipes with small constant-depth circumferential surface cracks subject to the tensile loading based upon the General Electric/Electric Power Research (GE/EPRI) method. The values of elastic influence functions for stress intensity factor and plastic influence functions for fully plastic J-integral are derived in tabulated forms through a series of three-dimensional (3D) finite element (FE) calculations for a wide range of crack geometries and material properties. Furthermore, the fit equations for elastic and plastic influence functions are developed, where the effects of crack geometries are explicitly revealed. The new influence functions lead to an efficient J estimation and can be well applied for structural integrity assessment of thin-walled pipes with small constant-depth circumferential surface cracks under tension. [DOI: 10.1115/1.4038226]

1 Introduction

The failure assessment of crack-like flaws is an important issue in design and maintenance of piping systems, including nuclear power plants, oil and gas transmission pipelines, and marine risers. Specifically, the fracture parameter, *J*-integral, has been widely used in the structural integrity assessment of defective pipes. Full three-dimensional (3D) finite element (FE) analyses can provide accurate results for the fracture response. However, FE analyses require large computational time, expertise, and resources, which make the numerical computation quite expensive to be used routinely; hence, they are not suitable for engineering structural integrity assessment. Therefore, the simplified *J*-estimation scheme with much less computational cost is highly desired from view of engineering application.

Based upon the fully plastic *J*-integral solution developed by Shih and Hutchinson [1], Kumar et al. [2] introduce the widely known General Electric/Electric Power Research (GE/EPRI) *J* estimation approach for two-dimensional geometries. Afterward, the original work was extended by various researchers [3–12] to include additional geometries and loading conditions. Another popular *J*-estimation method is the reference stress approach, which adopts the plastic limit load as the reference stress [13]. Based upon the FE results for pipes with varying geometries under different loading conditions, it was proposed that the reference stress can be redefined by an "optimized reference load" (rather than the plastic limit load) [14–17]. This method is termed as enhanced reference stress method and can improve the accuracy in *J*-estimation. However, it should be noted that these works mainly cover the cases of cracked pipes having mean diameter-to-thickness ratio (D/t) not more than 40.

The growing demand for energy and natural resources has been pushing exploration and production activities of oil and natural gas. In particular, application of thin-walled high strength steel has become a trend in the oil and gas transportation system over long distance, which can improve the transportation efficiency by high pressure operation and reduce the pipe laying cost by reducing the wall thickness of pipes. To verify the applicability limit of the existing GE/EPRI method with regard to the diameter-to-

[1]Corresponding author.

Contributed by the Pressure Vessel and Piping Division of ASME for publication in the Journal of Pressure Vessel Technology. Manuscript received December 18, 2016; final manuscript received September 28, 2017; published online November 30, 2017. Assoc. Editor: David L. Rudland.

thickness ratio D/t, Cho et al. [18] has explored the J-estimation schemes for semi-elliptical surface cracked pipes with D/t ranging from 10 to 120. Extensive 3D FE analyses were conducted for pipes with varying crack size (crack depth to pipe thickness ratio $a/t = 0.25$, 0.5, 0.75 and crack angle $\theta/\pi = 0.1$, 0.2, 0.3), material properties (strain hardening exponent $n = 1$, 3, 5, 10) [18]. Park et al. [19] have performed several FE analyses for pipes with a short circumferential through-wall crack. As pointed by those previous works [18–20], an application of existing solutions would result in inaccurate structural integrity assessment results when thin-walled pipes are considered. If existing GE/EPRI solution, whose applicability is $D/t \leq 40$, is extrapolated to thin-walled pipes with $D/t = 60$, the J-integral would be nonconservative comparing with the FE results [18,19]. Underestimation of the crack driving force is very dangerous in the engineering failure assessment, which needs to be avoided. Therefore, extension of the estimation methods is urgently required for thin-walled pipes. Furthermore, in most of previous works, the surface cracks are usually modeled as elliptical configuration. The long distance, oil and gas pipes are joined by weld. Common failures in pipelines result primarily from the weld defects. The surface cracks with constant depth might represent well the weld defects commonly observed in pipelines [21]. Moreover, based upon the limits routinely adopted in design as well as nondestructive testing examination, such as API 1104 [22], small cracks are often a major concern for the welded pipes with large diameter. In this content, an enhanced J estimation scheme for thin-walled pipes with small constant-depth cracks needs to be developed to overcome the limitations of the existing solutions.

A series of elastic and elastic–plastic FE analyses for the thin-walled pipes having D/t ranging from 50 to 100 under tension are conducted in this paper. The analyses involve small constant-depth cracks with crack depth-to-thickness ratio ranged 0.15–0.45 and crack length-to-thickness ratio ranged 4–32 for pipes with different strain hardening properties. By analyzing the FE results, the values of elastic influence functions for elastic stress intensity factor K and plastic influence functions for J-integral are proposed in tabulated forms based upon GE/EPRI estimation method. Furthermore, simple equations for elastic and plastic functions are developed, which makes the J estimation more efficient. To show the efficiency of the estimation method, J-integral values obtained from the newly proposed equations for the elastic and plastic influence functions are compared with those from detailed three-dimensional FE analyses.

2 The General Electric/Electric Power Research Method for J Estimation

To estimate elastic–plastic J-values for a cracked body, the GE/EPRI engineering method [1,2] was developed based on finite element solutions using deformation plasticity theory. The method assumes that the constitutive law for the materials can be characterized by the Ramberg–Osgood model

$$\frac{\varepsilon}{\varepsilon_0} = \frac{\sigma}{\sigma_0} + \alpha\left(\frac{\sigma}{\sigma_0}\right)^n \tag{1}$$

where σ is the true stress, ε is the true strain, σ_0 is the yield stress, E is the elastic modulus, $\varepsilon_0 = \sigma_0/E$ is the corresponding reference strain, α is a dimensionless constant and n defines the strain hardening exponent.

The GE/EPRI estimation method evolved from the two limiting cases of elastic and fully plastic conditions. The elastic–plastic J-integral is split into elastic and plastic components, as

$$J = J_e(a_e) + J_p \tag{2}$$

where the subscript "e" denotes the elastic part of J, adjusted by a plastic zone correction using the effective crack length a_e, and "p" refers to plastic contributions.

The elastic component J_e can be expressed via the stress intensity factor K by

$$J_e(a_e) = \frac{K(a_e)^2}{E'} \tag{3}$$

where $E' = E$ for plane stress condition and $E' = E/(1-\nu^2)$ for plane strain condition with ν representing the Poisson's ratio. Based on a modified Irwin plastic zone correction, the effective crack length a_e is defined as [7]

$$a_e = a + \frac{1}{(1+P/P_L)^2}\frac{1}{\beta\pi}\left(\frac{n-1}{n+1}\right)\left(\frac{K(a)}{\sigma_0}\right)^2 \tag{4}$$

where a is the crack length, P_L is the plastic limit load of the cracked component, $\beta = 2$ for plane stress, and $\beta = 6$ for plane strain conditions. For circumferential surface cracked pipes under tension, the expression for elastic stress intensity factor K can be given by Ref. [23]

$$K = \frac{P}{\pi Dt}\sqrt{\pi a}F \tag{5}$$

where F is the elastic influence function and P is the axial tensile loading.

In 1976, Shih and Hutchinson [1] developed a new method for fully plastic J-integral solutions. Upon consideration of a fully plastic cracked structure in which the elastic strains ε_e are vanishingly small compared with the plastic strains ε_p, the material defined by Eq. (1) follows a pure power-law stress–strain curve:

$$\frac{\varepsilon_p}{\varepsilon_0} = \alpha\left(\frac{\sigma}{\sigma_0}\right)^n \tag{6}$$

Under such assumption and close to the crack tip, the crack tip stress fields are given by the Hutchinson–Rice–Rosengren (HRR) singularity [24,25]

$$\frac{\sigma_{ij}}{\sigma_0} = \left(\frac{J_p}{\alpha\sigma_0\varepsilon_0 I_n r}\right)^{\frac{1}{n+1}}\tilde{\sigma}_{ij}(n,\varphi) \tag{7}$$

where (r, φ) are polar coordinates centered at the crack tip, I_n is an integration constant, and $\tilde{\sigma}_{ij}(n,\varphi)$ are dimensionless stress functions. The HRR equation can be rewritten in the form of J-integral [23]

$$J_p = \alpha\sigma_0\varepsilon_0 I_n r\left(\frac{\sigma_{ij}}{\sigma_0}\right)^{n+1}\tilde{\sigma}_{ij}^{n+1} \tag{8}$$

With the application of Ilyushin's theorem [26] that the fully plastic stresses are simply proportional to the applied load P, the fully plastic J given by Eq. (8) can be expressed in terms of the applied load

$$J_p = \alpha b\sigma_0\varepsilon_0 h_1\left(\frac{P}{P_{\text{ref}}}\right)^{n+1} \tag{9}$$

where $b = t - a$ defines the uncracked ligament and h_1 is the plastic influence function dependent on crack size, specimen geometry, and strain hardening exponent. In Eq. (9), the load is normalized by a reference load P_{ref}, which may be freely chosen provided it is proportional to σ_0 but is often identified with the plastic limit load of the cracked component.

3 Finite Element Analysis

Consider a surface cracked pipe with mean diameter D and thickness t as shown in Fig. 1. The circumferential surface crack

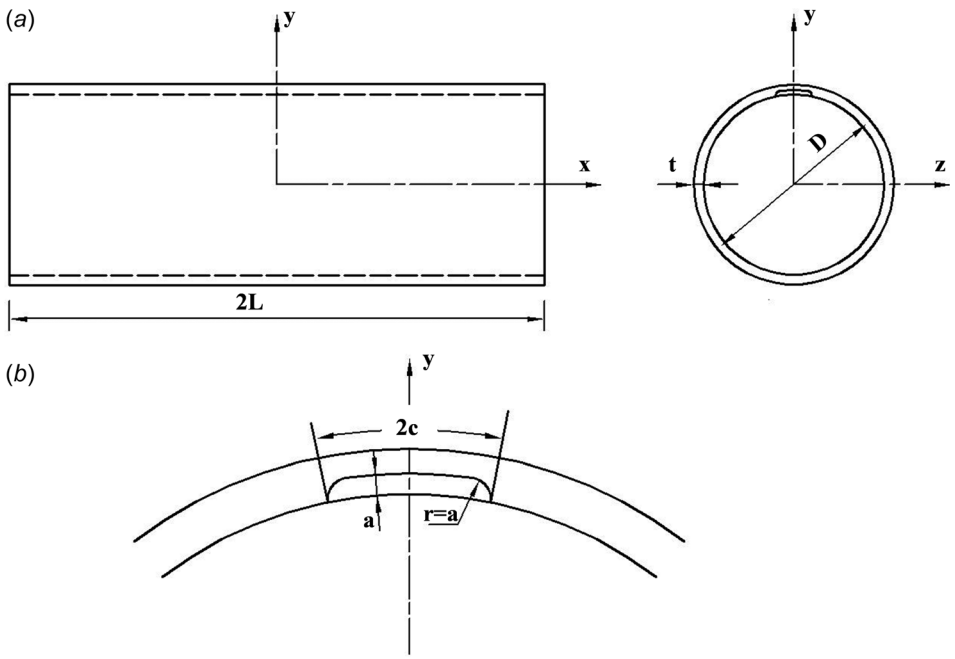

Fig. 1 (*a*) The geometrical dimension of the pipe with a circumferential surface crack and (*b*) geometry of the constant depth surface crack

in this work is assumed to be of constant depth a and length $2c$ with an end radius equal to the crack depth (as displayed in Fig. 1). For the thin walled pipe with large diameter, half of total circumferential crack angle θ is related to the crack length by

$$\theta = 2c/D \tag{10}$$

The thin walled pipes with large diameter are of main concern; here, three typical diameter-to-thickness ratios are considered, namely, $D/t = 50$, 75, and 100. First, the diameter-to-thickness ratio $D/t = 75$ is adopted for the simulations. The mean radius D and wall thickness t are taken as 1222.5 mm and 16.3 mm, respectively. According to the limits routinely adopted in design as well as nondestructive testing examination for the welded pipelines with large diameter, the values of crack depth-to-thickness ratio a/t are rationally selected as $a/t = 0.15$, 0.25, 0.35, and 0.45, and the half crack length-to-crack depth ratio c/a are chosen to be 2, 4, 6, 8, 10, 12, and16 ($0.0025 \leq \theta/\pi \leq 0.0611$ for $D/t = 75$, see Eq. (10)) in this work. Further, thin-walled pipes having $D/t = 50$ and 100 with the same fixed wall thickness are also performed to examine the effect of radius-to-thickness ratio on J-integral. To make the end effects on the computed fracture parameter J-integral negligible, the total length of the pipe segment $2L$ is assumed to be six times the outer diameter [21].

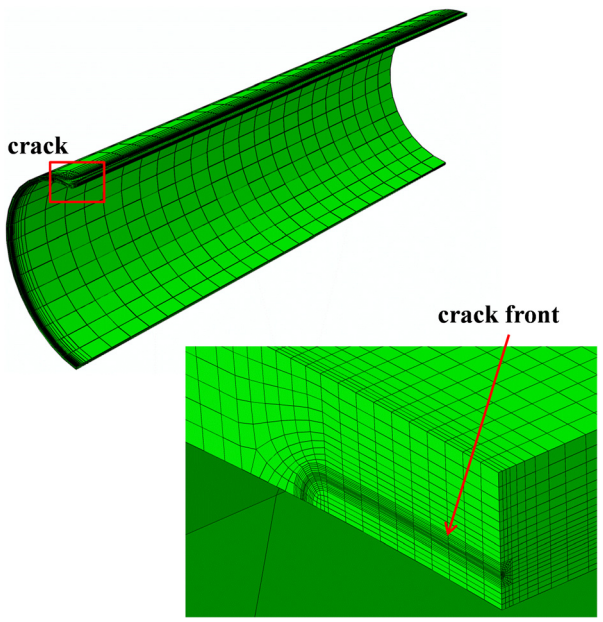

Fig. 2 Finite element mesh for the pipe with $a/t = 0.25$, $c/a = 8$ and $D/t = 75$

In this paper, all analyses were performed by the commercial FE program, ABAQUS [27]. A typical finite element mesh for the pipe with $a/t = 0.25$ and $c/a = 8$ is shown in Fig. 2. Considering the symmetry conditions, only one quarter of the pipe was modeled to improve the computational efficiency. Twenty-node isoparametric quadratic brick elements with reduced integrations (C3D20R within ABAQUS) were employed forming focused meshes around the crack tip. In order to reduce the singularities near the crack tip, a blunt crack front is modeled with a radius of 25 μm. Similar meshes were employed for models with other crack depths and crack lengths.

Symmetry boundary conditions were prescribed on the two surfaces whose normal direction is z-axis ($z = 0$ in Fig. 1(*a*)) as well as on the midsection of the pipe ($x = 0$ in Fig. 1(*a*)), except the crack face. The pipe was loaded in axial tension by specifying displacement to a reference node, which was tied to the uncracked end of the pipe via the multipoint constraint option within ABAQUS. The tensile load of the pipe P was determined from the force acting on the reference point.

Elastic and elastic–plastic FE analyses were performed to calculate the elastic fracture parameter K and the elastic–plastic fracture parameter J-integral. For elastic analyses, an isotropic material was assumed with Young's modulus $E = 200$ GPa and Poisson's ratio $\nu = 0.3$. For elastic–plastic analyses, the material was assumed to follow the Ramberg–Osgood relation described by Eq. (1). In this work, yield stress and dimensionless constant are fixed to $\sigma_0 = 650$ MPa and $\alpha = 0.5$. Different values of the strain-hardening index n are chosen ($n = 5$, 10, and 15) to perform parametric analysis. The value of hardening exponent $n = 5$ represents the high hardening material, $n = 10$ represents the medium hardening material and $n = 15$ is corresponding to the low

hardening material. In particular, the behavior of the material with $n = 5$ is in line with pipeline steel of grade API 5 L X52, the hardening exponent of $n = 10$ corresponds to pipeline steels of grade API 5 L X60–X65, and $n = 15$ represents API 5 L X70 or above [12,28].

The values of J-integral were calculated from the FE results using a domain integral method, as a function of applied tension loading. Noting that the overall deviation of the J-integral values, respectively, calculated from ten contours was less than a few percent, the confidence of the FE results was gained by the path independence of the J-integral values. Thus, the J-integral values were calculated from the mean of second to tenth contours after excluding the one immediately surrounding the crack tip. For the circumferential surface cracks with constant depth, the values of J-integral were extracted at the center of the crack. For elastic analyses, the calculated J-integral values were converted to elastic fracture parameters K by Eq. (3).

To make further confidence in the accuracy of the numerical results, elastic and plastic FE results were compared with existing solution. For constant depth surface crack, the applicability of Zahoor's solution [3] is $10 \le D/t \le 20$ and $0.05 \le \theta/\pi \le 1$. Figure 3 shows comparisons of F values obtained from the FE analyses and Zahoor's solution [3] for pipes with $a/t = 0.45$ and $\theta/\pi = 0.05$. Figure 4 compares the numerical J-integral values by detailed FE analysis with Zahoor's solution [3] and similar results provided by Cho et al. [18] for relatively thick-walled pipes with $D/t = 20$, $a/t = 0.25$ and $\theta/\pi = 0.1$. As shown in Fig. 3, the difference between the values of elastic influence function F from FE analyses and those from Zahoor [3] is minor when D/t is around 20. The J-integral values from FEA, Zahoor [3], and Cho et al. [18] are found to be consistent with each another for the relatively thick-walled pipe with $D/t = 20$ as displayed in Fig. 4. Therefore, the FE analyses are sufficiently validated for this study. On the other hand, it can be seen from Fig. 3 that the deviation of the elastic influence function F by FE analyses from those of Zahoor [3] increases with the growth of D/t for pipes with $D/t > 20$, which means new elastic influence function needs to be proposed for the application to the thin-walled pipes. To check the applicability of existing GE/EPRI method with regard to D/t, elastic–plastic FE analysis is also carried out for thin-walled pipe with $D/t = 100$. Figure 5 shows comparisons of J-integral versus applied load obtained from the FE analyses and Zahoor's solution [18] for thin-walled pipe with $D/t = 100$, $a/t = 0.45$ and $\theta/\pi = 0.05$. As shown in Fig. 5, the existing GE/EPRI solution underestimates the J-integral when thin-walled pipes with small cracks are considered. Therefore, extension of existing GE/EPRI method is conducted in Sec. 4 for the thin-walled pipes with small cracks.

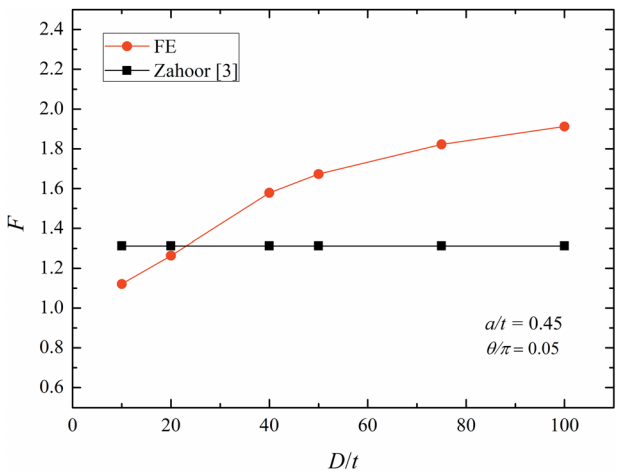

Fig. 3 Comparison of F values for pipes with $a/t = 0.45$ and $\theta/\pi = 0.05$

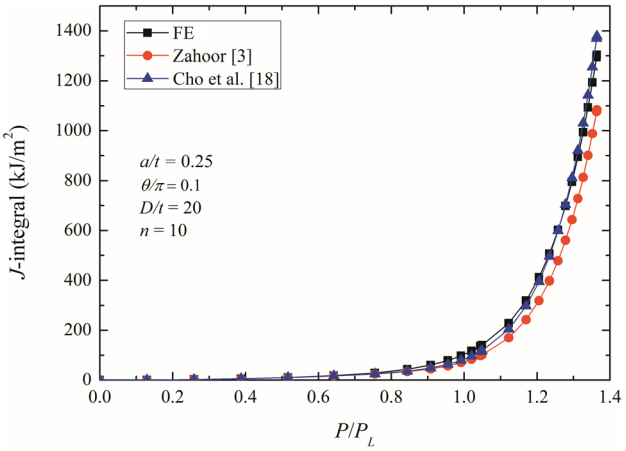

Fig. 4 Comparison of J-integral values for relatively thick-walled pipes with $D/t = 20$, $a/t = 0.25$ and $\theta/\pi = 0.1$

4 Results and Discussion

4.1 New Elastic Influence Function F. For the thin-walled pipes with diameter-to-thickness ratio $D/t = 75$, the values of F for the stress intensity factor resulting from the elastic FE analyses are given in Table 1. Based upon the FE results, it was found that the dependence of F on crack depth-to-thickness ratio ($a/t \le 0.45$) and half crack length-to-depth ratio ($c/a \le 16$) can be well fitted by the following equation:

$$\begin{aligned} F(a/t, c/a) &= M_1 + M_2(a/t)^2 + M_3(a/t)^4 \\ M_1 &= -0.376(c/a)^{-1} + 1.093 \\ M_2 &= -7.344(c/a)^{-0.436} + 6.033 \\ M_3 &= \frac{-0.681(c/a)^2 - 18.052(c/a) + 33.875}{(c/a)^2 + 2.704(c/a) + 3.168} \end{aligned} \tag{11}$$

Figure 6 shows the values of F resulting from the FE results and the proposed Eq. (11). For the thin-walled pipes with small circumferential surface cracks, it can be seen that the newly proposed equation describes the elastic influence function F satisfactorily.

4.2 New Plastic Influence Function h_1. In order to give the J estimation, the calculation of the plastic influence function h_1 follows an evaluation procedure. First, the plastic component of J

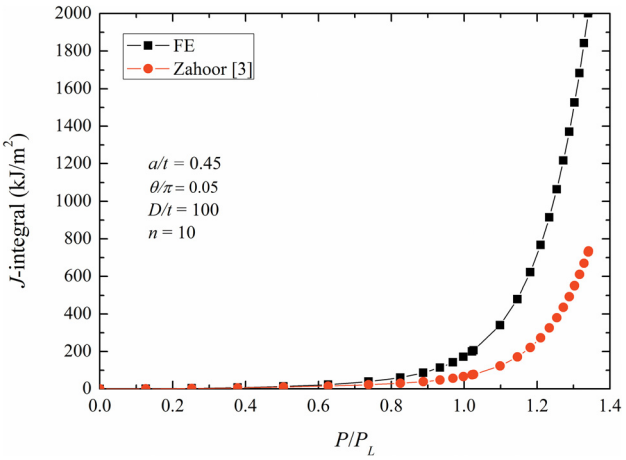

Fig. 5 Comparison of J-integral values for thin-walled pipes with $D/t = 100$, $a/t = 0.45$ and $\theta/\pi = 0.05$

Table 1 Tabulated values of F for thin-walled pipes with $D/t = 75$ under tension

	c/a						
a/t	2	4	6	8	10	12	16
0.15	0.9194	1.5062	1.0974	1.1193	1.1331	1.1421	1.1553
0.25	0.9375	1.1154	1.1881	1.2306	1.2588	1.2778	1.3016
0.35	0.9723	1.2103	1.3260	1.3951	1.4421	1.4734	1.5118
0.45	1.0191	1.3299	1.4980	1.6044	1.6697	1.7168	1.7760

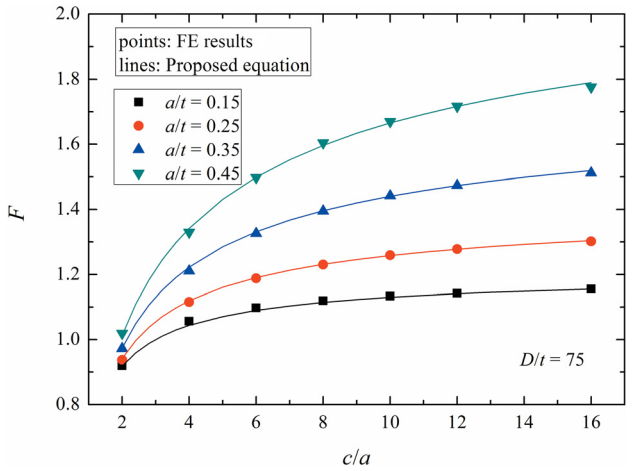

Fig. 6 Variation of F values, resulting from the FE results and the proposed equation, with c/a for pipes with $D/t = 75$

values was calculated by subtracting the elastic component from the total FE J values

$$J_p^{\mathrm{FE}} = J^{\mathrm{FE}} - \frac{1}{E}\left[\frac{P}{\pi Dt}\right]^2 \pi a_e F(a_e)^2 \tag{12}$$

where elastic function F was derived from the proposed analytical solution by Eq. (11). Then Eq. (9) was rewritten into the following form:

$$\bar{J}_p = \frac{J_p}{\alpha b \sigma_0 \varepsilon_0} = h_1 \left(\frac{P}{P_L}\right)^{n+1} \tag{13}$$

so that the values of h_1 can be determined from the slope of a least square fit to the linear evolution between normalized plastic component of J-integral, denoted $\bar{J}_p$ and $(P/P_L)^{n+1}$ [4,8]. For thin-walled pipes under tension, lower bounds to limit tension loads P_L based on equilibrium stress fields, are given by Ref. [29]

$$P_L = \kappa P_0 = \left[1 - \frac{\theta}{\pi}\frac{a}{t} - \frac{2}{\pi}\sin^{-1}\left(\frac{a}{t}\frac{\sin\theta}{2}\right)\right] P_0 \tag{14}$$

where P_0 is the limit load for the uncracked component, $P_0 = \pi D t \sigma_0$.

Figures 7–9 illustrate the procedure for computing plastic influence function h_1 from the linear variation of $\bar{J}_p$ with $(P/P_L)^{n+1}$ for circumferentially cracked pipes having $D/t = 75$ with strain hardening exponent $n = 5$, 10, and 15, respectively. These figures cover pipe specimens with $a/t = 0.15$ and 0.45, $c/a = 2$ and 8. The particular point given by $(P/P_L)^{n+1} = 1.0$ corresponds to the attainment of the limit tension loading for each analyzed configuration. When the applied load exceeds the limit tensile loading ($P > P_L$), the well contained near-tip elastic–plastic stress fields evolve into a fully plastic condition (in which the crack ligament has reached yielding). As displayed in these figures, for the selected pipe with small crack geometries and different material properties, a linear relationship between $\bar{J}_p$ and the applied loading $(P/P_L)^{n+1}$ exists on the entire loading level (from elastic–plastic condition to the fully plastic condition), which confirms the effectiveness of the plastic function h_1 in the J estimation procedure defined by Eq. (9). The slope of the $\bar{J}_p$–$(P/P_L)^{n+1}$ curve for the entire range of loading level was derived from the best fit and h_1 was gained from the slope.

Tables 2–4 list the values of plastic function h_1 for the circumferentially cracked pipes having $D/t = 75$ with varying crack geometries and material properties from the J estimation procedure previously outlined. To facilitate easy prediction of the J-integral and using the h_1 values represented in Tables 2–4, we built a mathematical model of h_1 incorporating parameters of a/t and c/a ($a/t \le 0.45$, $c/a \le 16$)

$$\begin{aligned} h_1(a/t, c/a) &= \{\varsigma_0 + \varsigma_1 (c/a)^{0.5} + \varsigma_2 (c/a)\} \\ \varsigma_0 &= \beta_1 (a/t)^{\beta_2} + \beta_3 \\ \varsigma_1 &= \beta_4 (a/t)^{\beta_5} + \beta_6 \\ \varsigma_2 &= \beta_7 (a/t)^{\beta_8} + \beta_9 \end{aligned} \tag{15}$$

By a standard least-square fitting to the h_1 data for each material property, Table 5 provides the coefficients of β_i ($i = 1$–9)

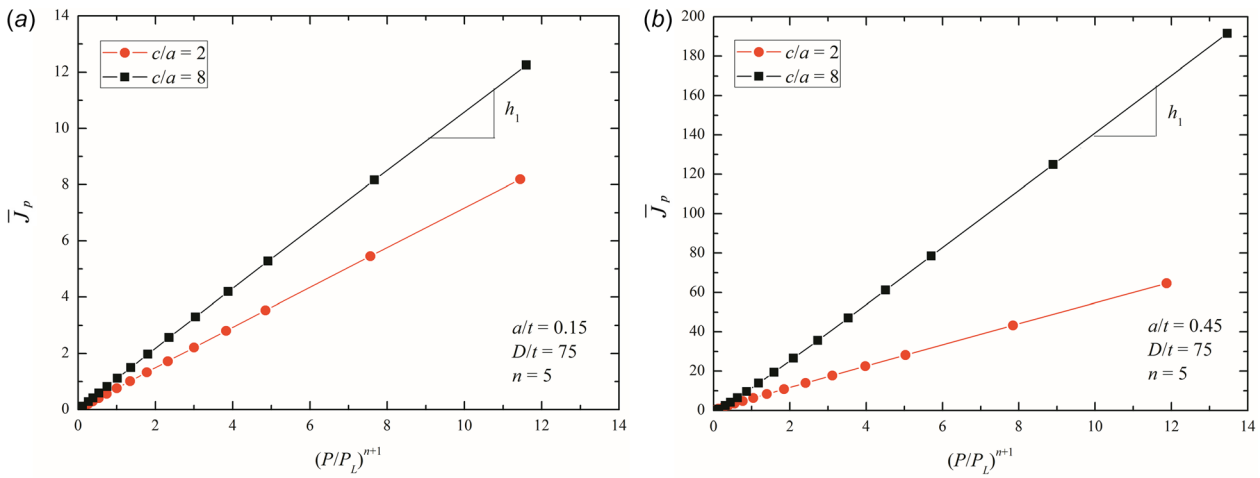

Fig. 7 Determination of h_1 factors from the linear variation of $\bar{J}_p$ with $(P/P_L)^{n+1}$ for the pipes with $n = 5$ and $D/t = 75$: (*a*) $a/t = 0.15$ and (*b*) $a/t = 0.45$

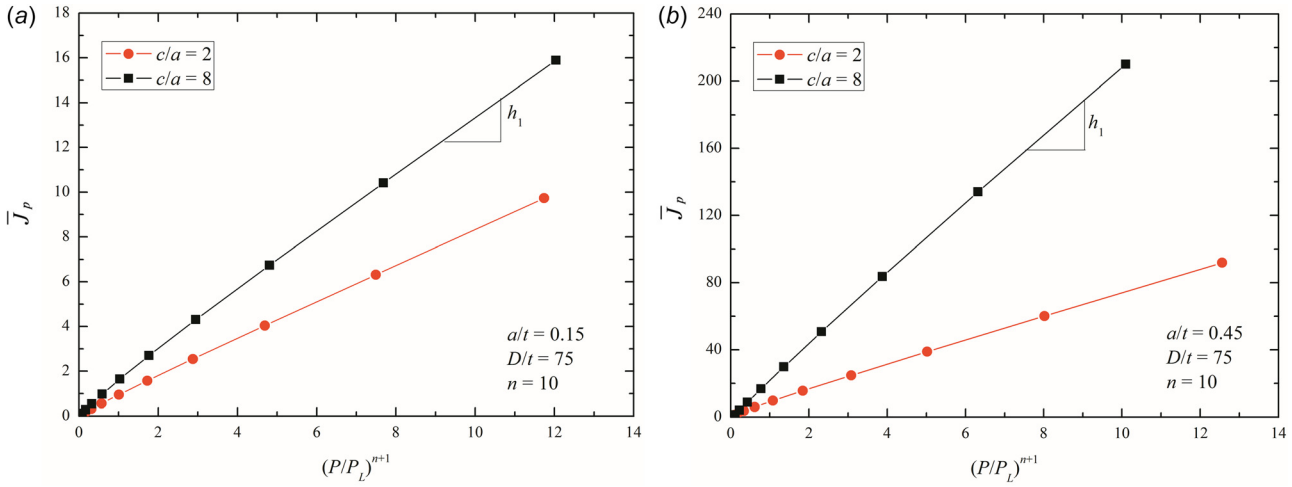

Fig. 8 Determination of h_1 factors from the linear variation of $\bar{J}_p$ with $(P/P_L)^{n+1}$ for the pipes with $n = 10$ and $D/t = 75$: (*a*) $a/t = 0.15$ and (*b*) $a/t = 0.45$

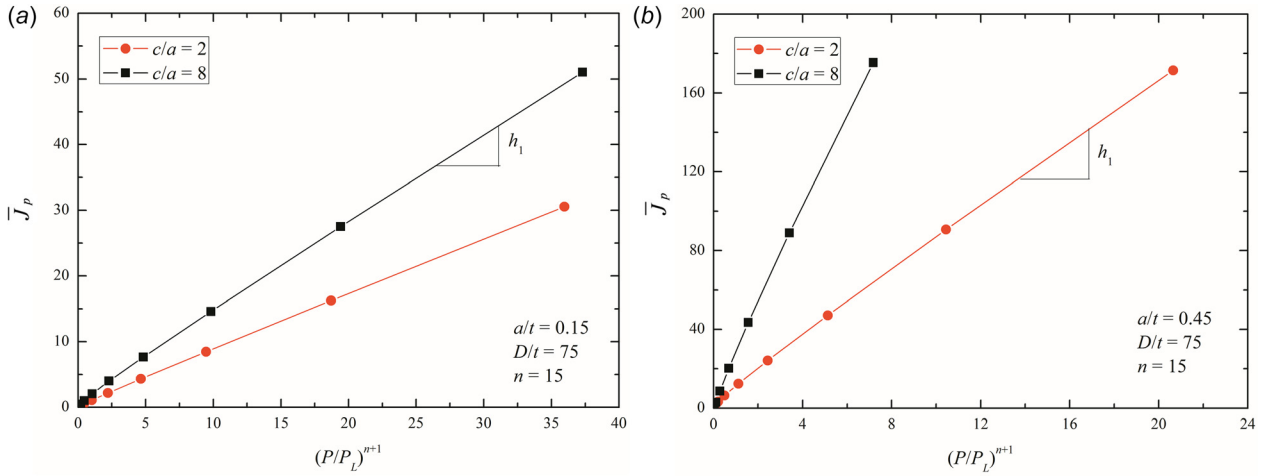

Fig. 9 Determination of h_1 factors from the linear variation of $\bar{J}_p$ with $(P/P_L)^{n+1}$ for the pipes with $n = 15$ and $D/t = 75$: (*a*) $a/t = 0.15$ and (*b*) $a/t = 0.45$

presented in Eq. (15). Figure 10 compares the values of h_1 derived from the FE results and the proposed equation for the thin-walled pipes with varying crack geometries and material properties, which represents effectiveness of the new proposed equation for the plastic influence function h_1.

By using the GE/EPRI method with proposed equations for the elastic and plastic influence functions, the elastic–plastic J-integral are estimated and compared with those from FE results. Figures 11–13 provide the comparison of estimated J-integral with FE results for thin-walled pipes having $D/t = 75$ with varying crack geometries and material properties. In Figs. 11–13, new GE/

Table 3 Tabulated values of h_1 for thin-walled pipes under tension with $D/t = 75$ and $n = 10$

	c/a						
a/t	2	4	6	8	10	12	16
0.15	0.8556	1.1448	1.2796	1.3986	1.4851	1.5472	1.6300
0.25	1.9136	3.0399	3.8015	4.3707	4.7822	5.0685	5.3738
0.35	3.9693	7.2581	9.6116	11.1868	12.3464	13.1358	13.7476
0.45	7.5968	14.1918	18.6984	21.3974	22.788	23.6476	23.9587

Table 2 Tabulated values of h_1 for thin-walled pipes under tension with $D/t = 75$ and $n = 5$

	c/a						
a/t	2	4	6	8	10	12	16
0.15	0.7293	0.9163	1.0191	1.0828	1.1222	1.1450	1.1664
0.25	1.5165	2.2126	2.6123	2.8852	3.0775	3.1764	3.2912
0.35	3.0288	4.9358	6.1676	6.9083	7.4312	7.7037	7.8393
0.45	5.5857	9.8652	12.6897	14.0002	14.4531	14.4706	13.4758

Table 4 Tabulated values of h_1 for thin-walled pipes under tension with $D/t = 75$ and $n = 15$

	c/a						
a/t	2	4	6	8	10	12	16
0.15	1.0489	1.4837	1.7392	1.9441	2.1015	2.2202	2.3637
0.25	2.4870	4.1573	5.4330	6.4028	7.1152	7.6405	8.2247
0.35	5.4068	9.9637	13.3332	15.7747	17.6607	18.9449	19.9475
0.45	10.4679	19.1862	25.0522	28.2734	30.0405	31.0974	30.6874

Table 5 Coefficients for the plastic function h_1 given by Eq. (15) for thin-walled pipes having $D/t = 75$

	Coefficient								
n	β_1	β_2	β_3	β_4	β_5	β_6	β_7	β_8	β_9
5	−251.0203	3.8193	0.2690	257.6138	3.5570	0.2393	−48.2150	3.8706	−0.0350
10	−453.1246	4.0271	−0.0177	445.5834	3.7899	0.5945	−127.7363	4.7786	−0.1045
15	−447.8969	3.6708	−0.3534	533.1161	3.6388	0.9573	−212.7676	4.9990	−0.1640

EPRI means the GE/EPRI method with newly generated elastic and plastic influence functions by fit equations. As shown in these figures, the results of GE/EPRI estimation method with new elastic and plastic influence functions agree well with the FE results.

Before exploring the effect of diameter-to-thickness ratio D/t on J-integral, a simple analysis is conducted. For the pipes with small cracks considered in this paper under tension, the applied load can be approximately related to the axial stress by

$$\frac{P}{P_0} = \frac{\sigma}{\sigma_0}$$
$$\frac{P}{P_L} = \frac{\sigma}{\sigma_L} = \frac{1}{\kappa(a/t, c/D)}\frac{\sigma}{\sigma_0} \tag{16}$$

As it can be seen from Eq. (16), for the pipes with the same a/t and c/a, the dimensionless load P/P_0 is independent on the diameter-to-thickness ratio D/t when the same axial stress σ/σ_0 is considered, while P/P_L is related to D/t by the parameter κ. Based upon the GE/EPRI method and Eq. (16), the J-integral can be expressed by

$$J = f\left(\frac{a}{t}, \frac{c}{a}, \frac{D}{t}, n, \frac{P}{P_L}\right) = f_1\left(\frac{a}{t}, \frac{c}{a}, \frac{D}{t}, n, \frac{P}{P_0}\right) \tag{17}$$

By three-dimensional FE analyses, the effect of diameter-to-thickness ratio D/t on J–P/P_0 relationship for thin-walled pipes with different strain hardening exponent is displayed in Figs. 14–16. Three values of $D/t = 50$, 75, and 100 are considered in these figures. It should be specified that the dimensionless load is P/P_0 rather than P/P_L in these figures to make that the pipes with different diameter-to-thickness ratio have the same nondimensional load P/P_0 once the axial stress σ/σ_0 is fixed. These figures show that for the thin-walled pipes with small circumferential surface cracks ($a/t \leq 0.45$ and $c/a \leq 16$), the diameter-to-thickness

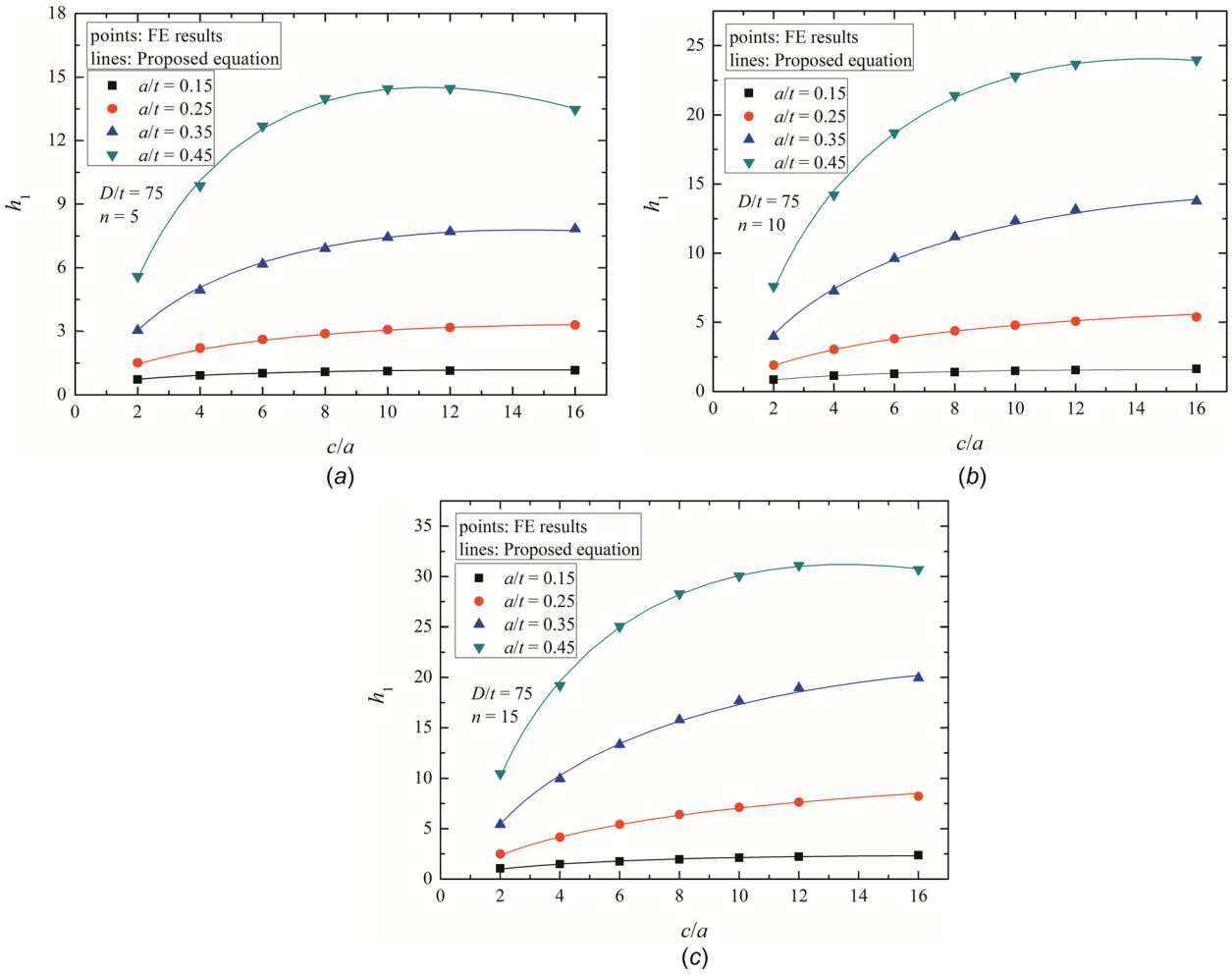

Fig. 10 Variation of the h_1 values, determined from the FE results and proposed equation, with c/a: (*a*) $n = 5$, (*b*) $n = 10$, and (*c*) $n = 15$

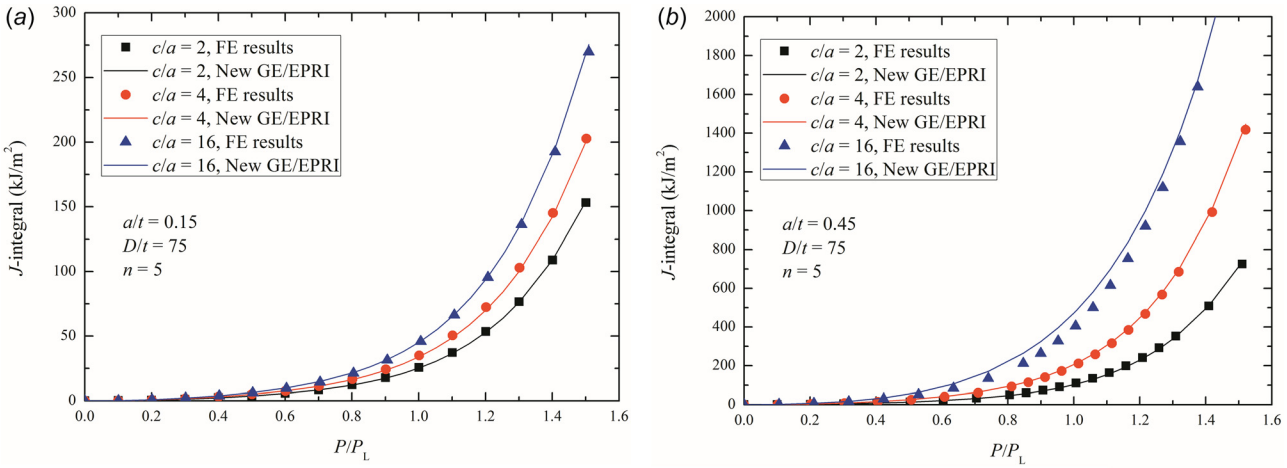

Fig. 11 Comparison of *J*-integral estimated by using new elastic and plastic influence functions with FE results for thin-walled pipes having $D/t = 75$ and $n = 5$: (*a*) $a/t = 0.15$ and (*b*) $a/t = 0.45$

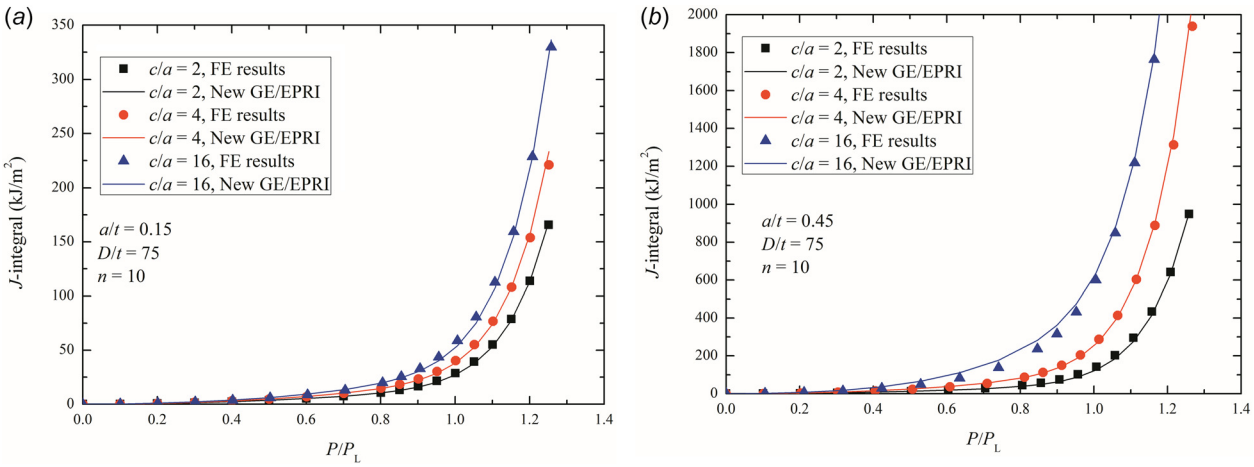

Fig. 12 Comparison of *J*-integral estimated by using new elastic and plastic influence functions with FE results for thin-walled pipes having $D/t = 75$ and $n = 10$: (*a*) $a/t = 0.15$ and (*b*) $a/t = 0.45$

ratio D/t ($50 \leq D/t \leq 100$) has a marginal effect on the J–P/P_0 relationship. This conclusion can be justified by the fact that the cracks considered in this paper are rather small compared to the pipe diameter and the variation of D/t is only from 50 to 100, in this case, the boundary effect due to variation of D/t can be neglected. Therefore, the engineering J estimation for varying diameter-to-thickness ratio D/t ranging from 50 to 100 can be simply obtained by the following procedures: (1) The diameter-to-thickness ratio D/t is assumed to be 75, variation of J with P/P_L is first estimated by the newly proposed elastic and plastic influence functions; then based upon the relationship between P_L and P_0 expressed by Eq. (14), the variation of J with P/P_0 for $D/t = 75$ is determined. (2) Considering the fact that for thin-walled pipes with small circumferential surface cracks ($a/t \leq 0.45$ and

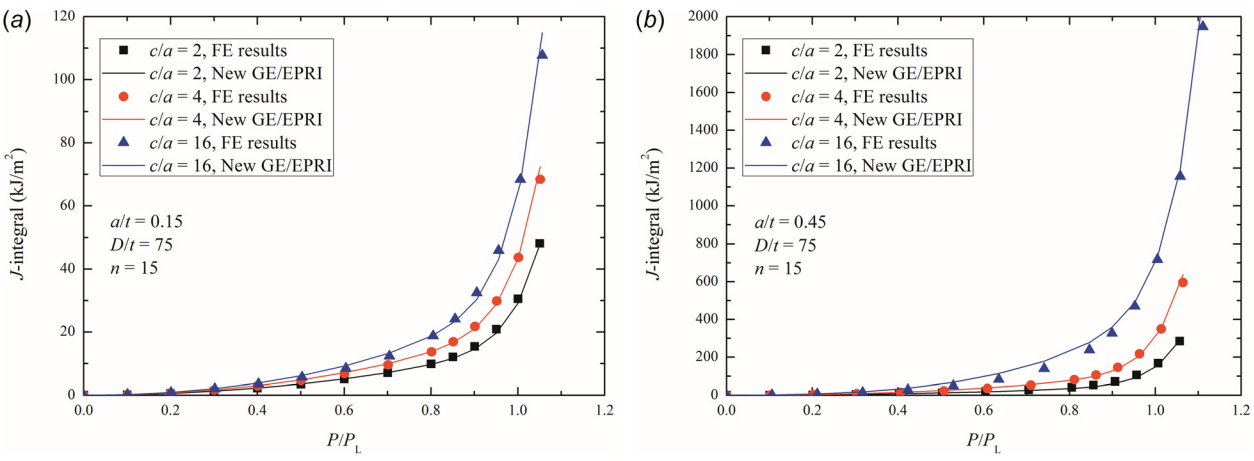

Fig. 13 Comparison of *J*-integral estimated by using new elastic and plastic influence functions with FE results for thin-walled pipes having $D/t = 75$ and $n = 15$: (*a*) $a/t = 0.15$ and (*b*) $a/t = 0.45$

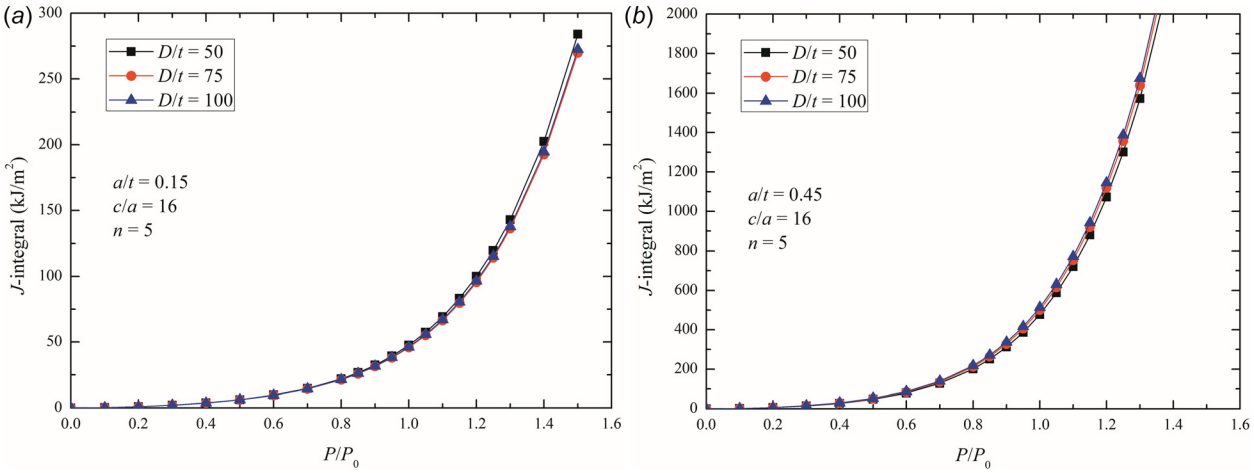

Fig. 14 The effect of D/t on J–P/P_0 relationship for thin-walled pipes with $n = 5$: (*a*) $a/t = 0.15$ and (*b*) $a/t = 0.45$

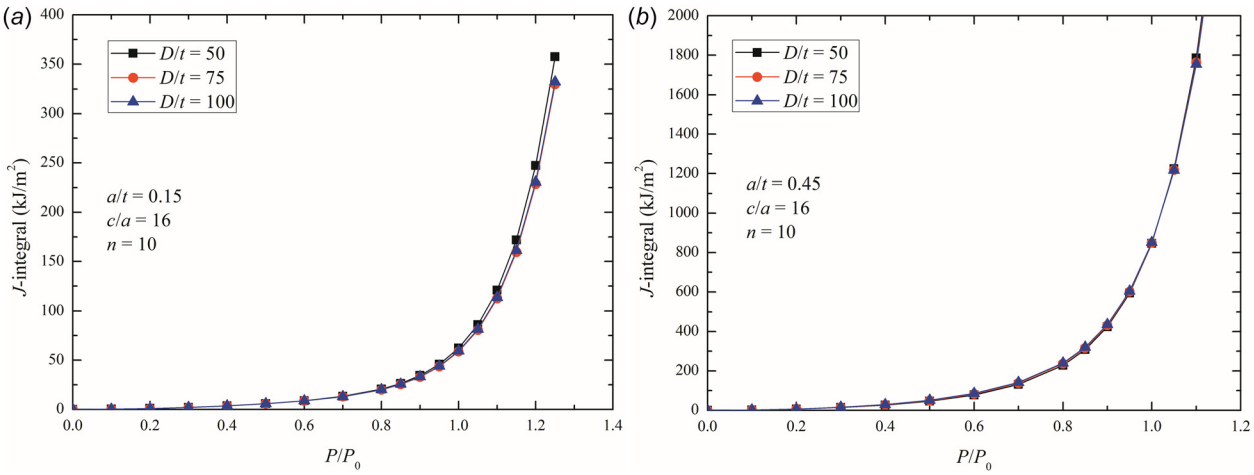

Fig. 15 The effect of D/t on J–P/P_0 relationship for thin-walled pipes with $n = 10$: (*a*) $a/t = 0.15$ and (*b*) $a/t = 0.45$

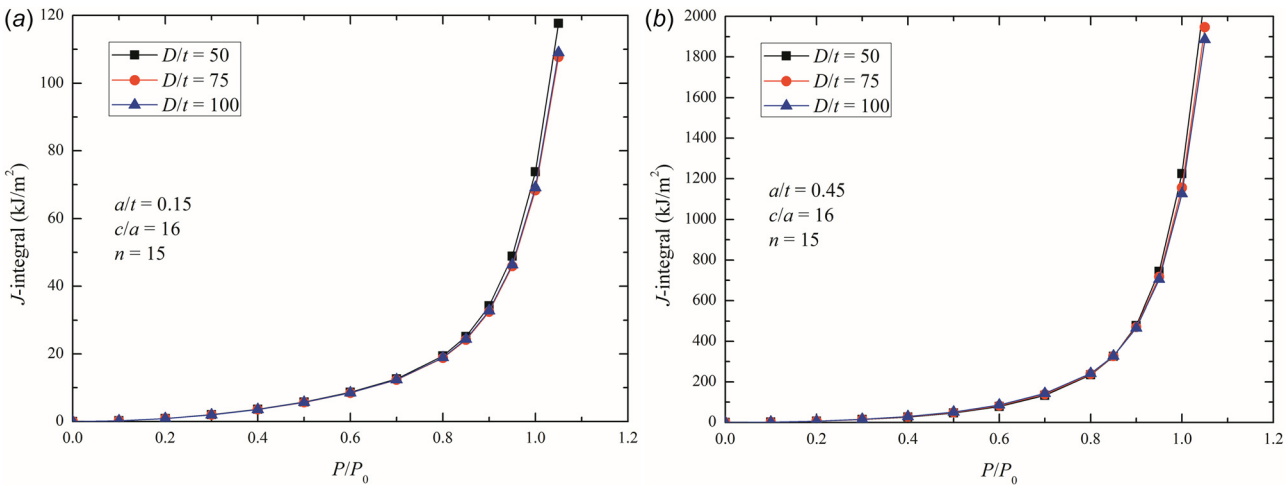

Fig. 16 The effect of D/t on J–P/P_0 relationship for thin-walled pipes with $n = 15$: (*a*) $a/t = 0.15$ and (*b*) $a/t = 0.45$

$c/a \leq 16$), the effect of diameter-to-thickness ratio D/t ($50 \leq D/t \leq 100$) on the J–P/P_0 relationship can be neglected, J-integral at different loading level of P/P_0 for varying diameter-to-thickness ratio D/t ranged 50–100 can be obtained by previous step.

5 Conclusions

This work provides a J estimation procedure for the thin-walled pipes with constant-depth circumferential surface cracks under

tensile loading based upon the GE/EPRI method. In this paper, attention is directed to the small cracks with constant depth having crack depth to pipe wall thickness ratio a/t ranging from 0.15 to 0.45, and half crack length over depth ratio c/a ranging from 2 to 16.

Three-dimensional FE analyses are conducted for the circumferential cracked pipes with a wide range of crack geometries and material properties in this paper. In the elastic FE analyses, FE values of the elastic influence function F are tabulated and a fit equation for F is proposed. By the elastic–plastic FE analyses, the values of the plastic influence function h_1 are derived and to facilitate easy prediction of the plastic influence function, a mathematical model for h_1 is developed. With newly proposed equations for the elastic and plastic influence functions, the GE/EPRI method can be successfully used to predict the J-integral for the thin-walled pipes with small circumferential surface cracks under tension.

Funding Data

- National Key Research and Development Program of China (Grant No. 2017YFB0702003).
- Nature Science Foundation of China (Grant Nos. 11132011, 11472287, 11402269, 11672299, and 11572324).
- Key Research Program of Frontier Sciences (Grant No. QYZDJSSW-JSC011).
- Strategic Priority Research Program of the Chinese Academy of Sciences (Grant Nos. XDB22040302 and XDB22040303).
- CAS/SAFEA International Partnership Program for Creative Research Teams.

Nomenclature

a = crack depth
a_e = effective crack length
b = uncracked ligament
c = half crack length
D = mean pipe diameter
E = Young's modulus
E' = "effective" Young 's modulus
f, f_1 = J-integral function
F = elastic influence function for elastic stress intensity factor
h_1 = plastic influence function for J_p in the GE/EPRI method
I_n = integration constant for HRR fields
J = J-integral
J_e = elastic component of J-integral
$\bar{J}_p$ = a normalization of J_P
J_p = plastic component of J-integral
J_p^{FE} = J_p obtained by FE analysis
K = elastic stress intensity factor
L = half pipe length
M_i = coefficients to compute elastic influence function
n = strain hardening exponent
P = axial load of a pipe
P_L = plastic limit load of the cracked pipe
P_{ref} = reference load of the cracked pipe
P_0 = plastic limit load of the uncracked pipe
r, φ = polar coordinates
t = pipe thickness
x, y, z = rectangular coordinates
α = dimensionless constant for Ramberg–Osgood material
β = 2 for plane stress; = 6 for plane strain
ε = strain
ε_0 = reference strain; = σ_0/E
ζ_i, β_i = coefficients to compute plastic influence function
θ = half of total circumferential crack angle
κ = P_L/P_0
ν = Poisson's ratio
σ = stress
σ_{ij} = stress components
$\tilde{\sigma}_{ij}$ = dimensionless stress functions for HRR fields
σ_0 = yield stress

References

[1] Shih, C. F., and Hutchinson, J. W., 1976, "Fully Plastic Solutions and Large-Scale Yielding Estimates for Plane Stress Crack Problems," ASME J. Eng. Mater. Technol., **98**(4), pp. 289–295.
[2] Kumar, V., German, M. D., and Shih, C. F., 1981, *An Engineering Approach for Elastic-Plastic Fracture Analysis*, Electric Power Research Institute, Palo Alto, CA.
[3] Zahoor, A., 1989, *Ductile Fracture Handbook*, Electric Power Research Institute, Palo Alto, CA.
[4] Chiodo, M. S. G., and Ruggieri, C., 2010, "J and CTOD Estimation Procedure for Circumferential Surface Cracks in Pipes Under Bending," Eng. Fract. Mech., **77**(3), pp. 415–436.
[5] Foxen, J., and Rahman, S., 2000, "Elastic-Plastic Analysis of Small Cracks in Tubes Under Internal Pressure and Bending," Nucl. Eng. Des, **197**(1–2), pp. 75–87.
[6] Kumar, V., German, M. D., Wilkening, W. W., Andrews, W. R., Delorenzi, H. G., and Mowbray, D. F., 1984, *Advances in Elastic–Plastic Fracture Analysis*, Electric Power Research Institute, Palo Alto, CA.
[7] Kumar, V., and German, M. D., 1988, *Elastic-Plastic Fracture Analysis of Through-Wall and Surface Flaws in Cylinders*, Electric Power Research Institute, Palo Alto, CA.
[8] Paredes, M., and Ruggieri, C., 2015, "Engineering Approach for Circumferential Flaws in Girth Weld Pipes Subjected to Bending Load," Int. J. Pressure Vessels Piping, **125**, pp. 49–65.
[9] Mohan, R., Krishna, A., Brust, F. W., and Wilkowski, G. M., 1998, "J-Estimation Schemes for Internal Circumferential and Axial Surface Cracks in Pipe Elbows," ASME J. Pressure Vessel Technol., **120**(4), pp. 418–423.
[10] Chattopadhyay, J., Tomar, A. K. S., Dutta, B. K., and Kushwaha, H. S., 2005, "Elastic-Plastic J and COD Estimation Schemes for Through wall Circumferentially Cracked Elbow Under in-Plane Closing Moment," Eng. Fract. Mech., **72**(14), pp. 2186–2217.
[11] Chattopadhyay, J., 2006, "Improved J and COD Estimation by GE/EPRI Method in Elastic to Fully Plastic Transition Zone," Eng. Fract. Mech., **73**(14), pp. 1959–1979.
[12] Parise, L. F. S., Ruggieri, C., and O'Dowd, N. P., 2015, "Fully-Plastic Strain-Based J Estimation Scheme for Circumferential Surface Cracks in Pipes Subjected to Reeling," ASME J. Pressure Vessel Technol., **137**(4), p. 041204.
[13] Ainsworth, R. A., 1984, "The Assessment of Defects in Structures of Strain-Hardening Material," Eng. Fract. Mech., **19**(4), pp. 633–642.
[14] Kim, Y. J., Kim, J. S., Lee, Y. Z., and Kim, Y. J., 2002, "Non-Linear Fracture Mechanics Analyses of Part Circumferential Surface Cracked Pipes," Int. J. Fract., **116**(4), pp. 347–375.
[15] Kim, Y. J., and Budden, P. J., 2002, "Reference Stress Approximations for J and COD of Circumferential Through-Wall Cracked Pipes," Int. J. Fract., **116**(3), pp. 195–218.
[16] Kim, Y. J., Kim, J. S., Park, Y. J., and Kim, Y. J., 2004, "Elastic-Plastic Fracture Mechanics Method for Finite Internal Axial Surface Cracks in Cylinders," Eng. Fract. Mech., **71**(7–8), pp. 925–944.
[17] Kim, N. H., Oh, C. S., Kim, Y. J., Kim, J. S., Jerng, D. W., and Budden, P. J., 2011, "Limit Loads and Fracture Mechanics Parameters for Thick-Walled Pipes," Int. J. Pressure Vessels Piping, **88**(10), pp. 403–414.
[18] Cho, D. H., Seo, H. B., Kim, Y. J., Chang, Y. S., Jhung, M. J., and Choi, Y. H., 2011, "Advances in J-Integral Estimation of Circumferentially Surface Cracked Pipes," Fatigue Fract. Eng. Mater. Struct., **34**(9), pp. 667–681.
[19] Park, J. S., Choi, Y. H., and Im, S., 2014, "Generation of Plastic Influence Functions for J-Integral and Crack Opening Displacement of Thin-Walled Pipes With a Short Circumferential Through-Wall Crack," Int. J. Pressure Vessels Piping, **117–118**, pp. 117–24.
[20] Cho, D. H., Woo, S. W., Chang, Y. S., Choi, J. B., Kim, Y. J., Jhung, M. J., and Choi, Y. H., 2010, "Enhancement of J Estimation for Typical Nuclear Pipes With a Circumferential Surface Crack Under Tensile Load," J. Mech. Sci. Technol., **24**(3), pp. 681–686.
[21] Jayadevan, K. R., Østby, E., and Thaulow, C., 2004, "Fracture Response of Pipelines Subjected to Large Plastic Deformation Under Tension," Int. J. Pressure Vessels Piping, **81**(9), pp. 771–783.
[22] API, 2013, "Welding of Pipelines and Related Facilities," American Petroleum Institute, Washington, DC, Standard No. API 1104.
[23] Anderson, T. L., 2005, *Fracture Mechanics: Fundamentals and Applications*, CRC Press, Boca Raton, FL.
[24] Hutchinson, J. W., 1968, "Singular Behaviour at the End of a Tensile Crack in a Hardening Material," J. Mech. Phys. Solids, **16**(1), pp. 13–31.
[25] Rice, J. R., and Rosengren, G. F., 1968, "Plane Strain Deformation Near a Crack Tip in a Power-Law Hardening Material," J. Mech. Phys. Solids, **16**(1), pp. 1–12.
[26] Ilyushin, A. A., 1946, "The Theory of Small Elastic-Plastic Deformations," Prikadnaia Matematica i Mekhanika, **10**, pp. 347–356 (in Russian).
[27] Hibbitt, H., Karlsson, B., and Sorensen, P., 2011, "ABAQUS Analysis User's Manual Version 6.10," Simulia-Dassault Systèmes, Providence, RI.
[28] Mostaghel, N., and Byrd, R. A., 2002, "Inversion of Ramberg-Osgood Equation and Description of Hysteresis Loops," Int. J. Nonlinear Mech, **37**(8), pp. 1319–1335.
[29] Kim, Y. J., Shim, D. J., Nikbin, K., Kim, Y. J., Hwang, S. S., and Kim, J. S., 2003, "Finite Element Based Plastic Limit Loads for Cylinders With Part-Through Surface Cracks Under Combined Loading," Int. J. Pressure Vessels Piping, **80**(7–8), pp. 527–540.